

Non-invasive method to image cerebral blood volume increases in acute ischemic stroke patients

A. J. Huang^{1,2}, L. An³, J. Hua¹, M. Donahue⁴, S. Warach³, and P. van Zijl¹

¹FM Kirby Research Center, Johns Hopkins University, BALTIMORE, MD, United States, ²Department of Biomedical Engineering, Johns Hopkins University, Baltimore, MD, United States, ³National Institute of Neurological Disorders and Stroke, National Institutes of Health, Bethesda, MD, United States, ⁴Department of Radiology, Vanderbilt University, Nashville, TN, United States

Introduction: Stroke is the third leading cause of death affecting approximately fifteen million people each year in the world⁽¹⁾. Acute ischemic stroke, caused by the occlusion of cerebral blood vessels by an arterial embolus or thrombus, accounts for approximately 85% of stroke cases⁽²⁾. Recent research has shown that thrombolysis treatment with tissue plasminogen activator (tPA) to restore blood flow can be useful for reducing tissue infarction when given within the first six hours post-onset⁽³⁾. However, the benefit of tPA must be weighed against the risk of intracranial hemorrhage⁽⁴⁻⁶⁾, which occurs in ~5% of cases in which patients are treated with tPA and frequently leads to irreversible damage. The ability to quickly assess which patients may benefit from tPA is critical to improving clinical outcome and minimizing long-term disability. In the early stages of ischemia, blood pH reduces⁽⁷⁻⁸⁾, which leads to relaxation of smooth muscle cells and an increase in microvascular cerebral blood volume (CBV)⁽⁹⁻¹²⁾. However, such autoregulation is eventually exhausted, and the blood vessels collapse. Our hypothesis is that patients with regions of increased CBV have not yet exhausted autoregulatory mechanisms and could benefit from thrombolysis. Vascular Space Occupancy (VASO) MRI uses blood nulling to assess changes in CBV. Here we explore the feasibility of using Magnetization Transfer (MT-VASO) to visualize tissue at risk of infarction in acute cerebral ischemia.

Methods: Simulations were performed using the VASO model in Donahue et al⁽¹³⁾ to determine how the VASO signal intensity would change for various increases in CBV (Table 1). Five patients with confirmed acute cerebral ischemia were consented and scanned on a Philips 3T Achieva Scanner with body-coil excitation and an 8-channel SENSE receive coil. All were imaged between 0 and 7 hours after ischemic onset and scanned prior to treatment with tPA. MT-VASO⁽¹⁴⁾, a variation of VASO with higher signal-to-noise, was used to acquire images weighted by CBV. Diffusion tensor images (DTI), fluid attenuated inversion recovery (FLAIR), and dynamic susceptibility contrast-based (DSC) perfusion weighted images (PWI) were also acquired. Individual scan parameters were: FLAIR: 1x1x3.5 mm³, TI/TR/TE = 2600/9000/120 ms; PWI: 3x3x7 mm³, 80 dynamics, TR/TE = 1000/25; DTI: 2x2x3.5 mm³, b-value = 1000, 16 directions, TR/TE = 4418/62 ms; MT-VASO: 2x2x3.5 mm³, 240 ms MT pulse (B1 = 2 μ T, offset frequency -30 ppm), TI/TR/TE = 1081/6000/14 ms, scan time: 2 min 45 s. Images from acute scan and 24-hr follow-up were motion-corrected and co-registered to DTI scans using CATNAP⁽¹⁵⁾. To allow for comparison between imaging modalities, we interpolated all scans to the same resolution (0.94 x 0.94 x 3.5 mm³). Since small reductions in VASO signal intensity may be difficult to see with the naked eye, we automated the data analysis as follows. First, a region-growing algorithm was generated to create a white matter (WM) mask. Then, a region in contralateral normal appearing white matter (CNAWM) was selected. Finally, a t-statistic map of the ipsilateral side was calculated to assess difference with respect to CNAWM. We also calculated the number of WM voxels in the whole brain that the PWI scan and VASO t-statistic method predict to be at risk of infarction: Number of PWI voxels was taken as the region of DWI hyperintensity subtracted from the region of PWI hyperintensity in WM; Number of VASO voxels was taken as the region of DWI hyperintensity subtracted from region of elevated VASO t-statistics in WM.

Table 2. Comparison of Number of Voxels from VASO and PWI at Risk of Infarction versus Number of Voxels that Actually Progressed to Infarction

	Patient 1	Patient 2	Patient 3	Patient 4	Patient 5	Total
VASO voxels in PWI in WM	1001	2865	1291	1901	2092	9150
PWI voxels in WM	6104	12420	14049	13184	17380	63137
Voxels Progressing to Infarction in WM	874	743	1426	1851	1560	6454

Results and Discussion: Figure 1 shows MRI images of a 62-year old male presenting with symptoms of cerebral ischemia who was scanned 2 hours and 11 minutes post-onset, but who did not eventually receive tPA. The acute FLAIR image (Fig. 1A), traditionally used to image anatomy, appeared normal. The isotropic diffusion weighted image (DWI) (Fig. 1B) had hyperintensities near the ventricles and in the posterior lobe signifying likely irreversible damage. A large area of hyperintensity in the mean transit time (MTT) image (Fig. 1C) implies a large region of tissue at risk of infarction. Interestingly, the VASO image (Fig. 1D) only showed a reduction of signal intensity in the region where a hyperintensity was observed on the DWI. The follow-up FLAIR image (Fig. 2A), which is usually used to confirm evidence of infarction, only has hyperintensities elongated tissue T1, which also confirms what we see in the follow-up FLAIR. Figure 3 compares t-statistical assessment applied to a MT-VASO scan of an age-matched healthy volunteer (Fig. 3A) and on another stroke patient (Fig. 3B). The healthy control shows relatively equal t-statistic values in both hemispheres. However, when comparing a region in the CNAWM in the stroke patient, the regions of reduced signal intensity on the ipsilateral side shows higher t-statistic values. Notice a region of higher t-statistics (red) on the contralateral side. We attribute this to partial volume effects with gray matter and CSF from the slice above it. We also compared the ipsilateral and contralateral hemispheres of five stroke patients over apparent diffusion coefficient, mean transit time, and t-statistic maps derived from the VASO image (Fig. 4). Our results confirm that the t-statistic values in the penumbra are sensitive to increases in microvascular CBV. Additionally, we compared the number of voxels with elevated t-statistic values and the number of voxels with elevated mean transit times to the number of voxels that progressed to infarction in the penumbra (Table 2). Our results show that the number of voxels predicted to progress to infarction by VASO is closer to the number of voxels that actually infarcted than what is predicted by the PWI scan.

Conclusion: Our results show that MT-VASO data can identify the ischemic penumbra based on vasodilation. However, one of the drawbacks of this method is that it can currently only be used in white matter. Partial volume effects of gray matter and CSF make it difficult to study gray matter. This method can be used to derive maps in white matter of the blood-volume ischemic penumbra potentially providing physicians an additional piece of information to help guide therapy in acute stroke patients.

Figure 1

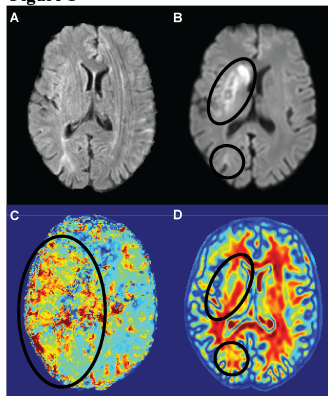


Figure 2

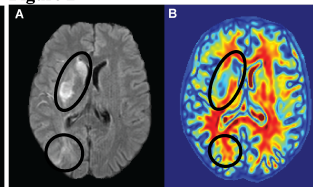


Figure 3

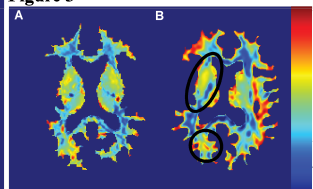


Figure 4

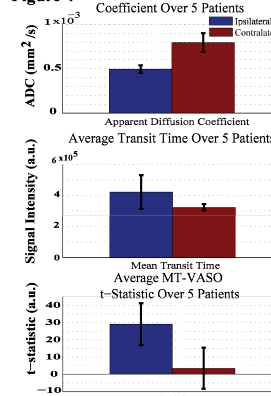


Figure 1. Images from acute stroke patient.

A. FLAIR B. DWI C. PWI (MTT) D. MT-VASO

Figure 2. 24-hr follow-up images for patient from Fig. 1

A. FLAIR B. MT-VASO

Figure 3. t-statistic maps of: A. Healthy age-matched control B. Patient

Figure 4. Comparison of Ipsilateral and Contralateral Hemispheres of Five Stroke Patients Using: A. ADC B. PWI-MTT C. MT-VASO t-statistic

References: (1) World Health Report 2002. (2) Rymer MM et al. *Neurol Res.* 2005;27 Suppl 1:S9-16. (3) Furlan A et al. *JAMA.* 1999;282(21):2003-11. (4) Brinker G et al. *Neuroreport.* 1999;10(9):1943-6. (5) Busch E et al. *JCBFM.* 1998;18(4):407-18. (6) Knight RA et al. *Stroke.* 1998;29(1):144-51. (7) Sorensen AG et al. *Radiology.* 1999;210(2):519-27. (8) Hatazawa J et al. *Stroke.* 1999;30(4):800-6. (9) Iadecola C. *Trends Neurosci.* 1997;20(3):132-9. (10) Gally JA et al. *PNAS.* 1990;87(9):3547-51. (11) Moro MA et al. *Cell Calcium.* 2004;36(3-4):265-75. (12) Back T

et al. *Ann Neurol.* 2000;47(4):485-92. (13) Donahue MJ et al *Magn Reson Med.* 2006;56(6):1261-73 (14) Hua J et al. *MRM.* 2009;61(4):944-51. (15) Landman BA et al. *Neuroimage.* 2007;36(4):1123-38. **Funding:** P41 RR 1524, R01EB004130